Int. J. Heat Mass Transfer. Vol. 27, No. 1, pp. 49–56, 1984
Printed in Great Britain

0017 9310/84 $3.00 + 0.00

NATURAL CONVECTION IN ENCLOSURES WITH OFF-CENTER INNERBODIES

E. M. SPARROW, P. C. STRYKER and M. A. ANSARI
Department of Mechanical Engineering, University of Minnesota, Minneapolis, MN 55455, U.S.A.

(*Received* 7 *March* 1983 *and in revised form* 27 *April* 1983)

Abstract—Measurements were made of the average Nusselt number at a small innerbody situated in an enclosed space, with the innerbody and the bounding wall of the enclosure maintained at different uniform temperatures. Natural convection occurred in the air which occupied the enclosed space. The position of the innerbody within the enclosure was varied parametrically, as was the orientation of the enclosure relative to the gravity field. Both the innerbody and the enclosure were cylinders with length–diameter ratios of unity, and the cylinder–cylinder diameter ratio was 0.2. At low Rayleigh numbers and for narrow gaps between the innerbody and the bounding wall of the enclosure, direct interwall conduction enhanced the innerbody Nusselt number. Aside from this, the Nusselt number was remarkably insensitive to both the position of the innerbody and the orientation of the enclosure. The results were correlated to within $\pm 6\%$ by the relation $Nu_i = 1.050\,Ra_i^{0.178}$.

NOMENCLATURE

A_i	surface area of inner cylinder
D	diameter of outer cylinder (equal to length)
D_i	diameter of inner cylinder (equal to length)
g	acceleration of gravity
H	length of outer cylinder
H'	interwall length for case (c), Fig. 1(c)
h_i	average inner-cylinder heat transfer coefficient
k	thermal conductivity
L	length from horizontal midpoint to extremity of outer cylinder
Nu_i	inner-cylinder Nusselt number
Pr	Prandtl number
Q_{conv}	convective heat transfer
Q_{rad}	radiative heat transfer
Ra_i	inner-cylinder Rayleigh number
T_i	inner-cylinder temperature
T_o	outer-cylinder temperature
X_c	horizontal coordinate
Z_c	vertical coordinate.

Greek symbols

β	coefficient of thermal expansion
ε_i	inner-cylinder emissivity
ν	kinematic viscosity
σ	Stefan–Boltzmann constant.

INTRODUCTION

NATURAL convection will occur in an enclosed space when the temperatures of bodies situated within the enclosure are different from that of the bounding wall. In recent years, there has been extensive study of natural convection in the space between an innerbody and the bounding wall of an enclosure, with primary emphasis on annuli bounded by spheres or by horizontal cylinders. The specific concern of the present work is with innerbodies that are positioned either off-axis, unsymmetrically, or eccentrically with respect to the bounding wall of the enclosure. Such positioning gives rise to nonuniformities of the gap between the innerbody and the enclosure wall.

Prior studies of heat transfer in the presence of off-center positioned innerbodies are reported in refs. [1–3]. The first of these dealt with spherical annuli made eccentric by displacing the inner sphere along the vertical diameter, while the second studied eccentric annuli between horizontal cylinders. The geometries of these cases are, respectively, axisymmetric and two-dimensional (2-D). In ref. [3], which is the forerunner of the present work, a three-dimensional (3-D) configuration was investigated experimentally, as will now be described.

The physical problem dealt with in ref. [3] is shown in Fig. 1(a), in both plan and elevation views. As shown, the enclosure is the space contained within a vertical cylinder whose height is equal to its diameter. The innerbody is also a vertical cylinder whose height and diameter are equal. The ratio of the diameter (height) of the inner cylinder to the diameter (height) of the outer cylinder is 0.2. As suggested in the diagram, the innerbody was placed at various positions in the enclosure during the course of the experiments, as specified by the two dimensionless coordinates of its center—the vertical coordinate Z_c/H and the horizontal coordinate X_c/L ($L = D/2 = H/2$). The temperatures of the inner and outer cylinders were maintained at different uniform values, with the temperature difference being varied parametrically.

A set of baseline experiments was performed for the axisymmetric case ($X_c/L = 0$) in which the inner-cylinder elevation was varied between $Z_c/H = 0.1375$ and 0.8625. The upper extreme position $Z_c/H = 0.8625$ is shown in the diagram, and the close proximity of the inner and outer cylinders is clearly in evidence. The lower extreme position corresponds to a similar

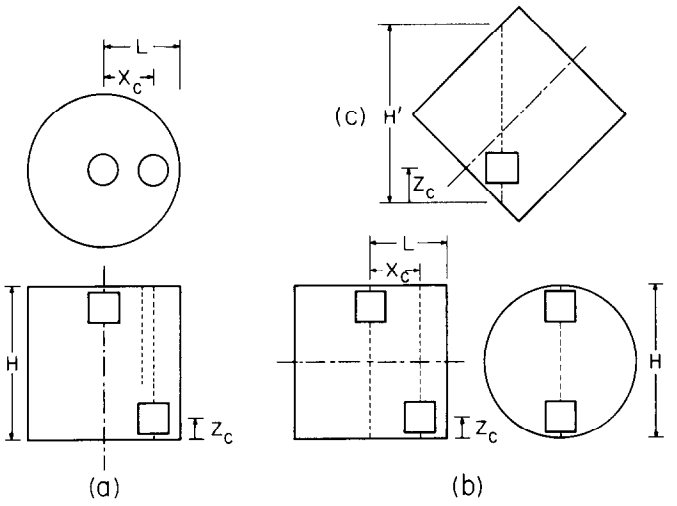

FIG. 1. Diagrams showing the various inner-cylinder positions and outer-cylinder orientations.

proximity of the cylinders. The experimentally determined Nusselt numbers for the axisymmetric case were in excellent agreement (typical deviation, 1%, extreme deviation, 3%) with those of finite difference solutions performed for $0.25 \leqslant Z_c/H \leqslant 0.75$.

Off-axis positioning was investigated by experiments in which the inner cylinder was displaced transversely to $X_c/L = 0.50$ and 0.65 and, at each transverse location, the elevation was varied between $Z_c/H = 0.1375$ and 0.8625. The lower extreme position at $X_c/L = 0.65$ is shown in the figure in order to illustrate the degree of proximity of the cylinders.

Despite the wide range of investigated inner-cylinder positions, the average Nusselt numbers corresponding to a given Rayleigh number were quite insensitive to position. An extreme elevation-related spread of 14% was encountered at the lowest investigated inner-cylinder Rayleigh number (~ 1500) for the axisymmetric case, but aside from this, position-related spreads in the 5–10% range were generally the rule, with the 5% value commonly prevailing for $Ra_i \geqslant 10^4$. This insensitivity is noteworthy in view of the significant position-related changes in the pattern of fluid flow in the enclosure (as given by the finite difference solutions for the axisymmetric case).

The just-described insensitivity served to motivate interest in determining the response of the average Nusselt number to even more severe misalignments of the two cylinders, and such an investigation is the focus of the present work. The strategy of the experimental program is displayed pictorially in Fig. 2. Figure 2(a) depicts the outer cylinder as it was situated during the experiments of ref. [3], i.e. with its axis vertical. In Fig. 2(b), the cylinder is seen in an inclined position with its axis at 45° to the vertical, while in Fig. 2(c), the cylinder axis is horizontal. The 45° and horizontal outer-cylinder orientations were employed during the course of the present experiments.

More definitive information about the inner-cylinder–outer-cylinder spatial relationships is presented in Figs. 1(b) and (c). Figure 1(b) shows an elevation view and an end view of the case where the axis of the outer cylinder is horizontal. As seen there, the inner cylinder is positioned with its axis vertical. Therefore, the axes of the two cylinders are misaligned by 90°, in contrast to the test setup of ref. [3] in which the axes of the cylinders are aligned [i.e. Fig. 1(a)]. Figure 1(b) also shows the coordinates X_c and Z_c which respectively specify the horizontal and vertical positions of the center of the inner cylinder. For illustrative purposes, the inner cylinder is shown at its upper extreme position ($Z_c/H = 0.8625$) at $X_c/L = 0$ and at its lower extreme position at $X_c/L = 0.65$.

Figure 1(c) shows the case where the axis of the outer cylinder is at 45° to the vertical, while the axis of the inner cylinder is vertical. The figure also shows the inner

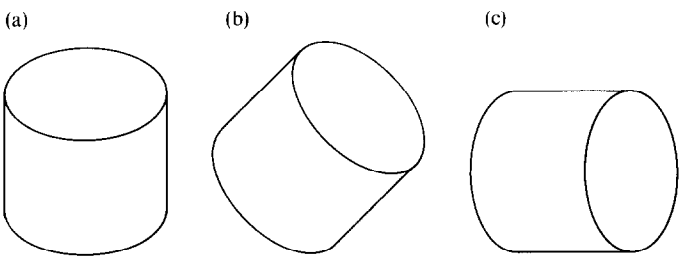

FIG. 2. Pictorial view of the investigated outer-cylinder orientations.

cylinder in its lower extreme position ($Z_c/H' = 0.2$), where one of its corners is in close proximity to one of the flat faces of the outer cylinder. In its upper extreme position ($Z_c/H' = 0.8$), a corner of the inner cylinder is in close proximity to the curved wall of the outer cylinder.

Average inner-cylinder Nusselt numbers will be determined for the various inner-cylinder–outer-cylinder configurations shown in Figs. 1(b) and (c). The fluid medium in the intercylinder space was air.

THE EXPERIMENTS

Apparatus and procedure

Since the present research is an extension of that of ref. [3], only an overall description of the apparatus is necessary. The main components of the apparatus include the outer cylinder, the inner cylinder, a platform which supports and orients the outer cylinder, and a large water bath which serves as the thermal environment for the outer cylinder.

The outer cylinder was made of 0.635 cm thick copper in order to aid the attainment of a spatially uniform wall temperature, which was verified by the readings of eleven wall-embedded thermocouples. After completion of all machining and finishing operations, the inside diameter and length of the cylinder, D and H, respectively, were both equal to 15.595 cm.

Two small apertures were machined into the cylindrical wall of the outer cylinder in order to permit passage of thermocouples, heater-wire leads, and a support line from the outside into the interior of the enclosure where they are attached to the inner cylinder. The apertures were used one at a time, and the one not in use was closed with a copper plug which was contoured to match the curvature of the inner surface of the cylindrical wall. The two apertures were situated in-line along the cylindrical wall at positions corresponding to $X_c/L = 0$ and 0.65 [see Fig. 1(b)], with $X_c = 0$ midway between the flat walls of the cylinder and with $L = H/2$.

To accommodate the fact that the outer cylinder was surrounded by water during the experiments, each aperture was fitted with a tube which passed vertically upward through the water and emerged into the air above the water surface. The inner-cylinder wires and support line passed through the tube bore and out into the air.

The inner cylinder was made of aluminum because of its high thermal conductivity and because it is capable of being polished to an enduring mirror-like surface finish (in contrast to copper, which tends to tarnish with time). The finished external diameter and length dimensions of the cylinder were 3.119 cm, which is exactly 20% of the corresponding dimensions of the outer cylinder. A cavity was machined into the cylinder to accommodate a specially wound electrical heating element. Two thermocouples were embedded in the cylinder walls, one at the top and one at the bottom. These thermocouples verified the attainment of temperature uniformity (to within the 1 μV read-out capability of the digital voltmeter).

The thermocouple wire, its diameter, and the diameter of the copper lead wire for the heating element were carefully selected from the standpoint of minimizing extraneous heat losses from (or to) the inner cylinder. The same concern prompted the use of a small-diameter cat-gut line for suspending the cylinder. A special self-centering fixture (contained within the cylinder) ensured that the cylinder always hung vertically. The vertical position of the inner cylinder (i.e. Z_c/H) was set by adjusting the length of the cat-gut line that passed into the enclosure, with the line length being measured with a vernier-equipped caliper.

Support for the outer-cylinder–inner-cylinder assembly was provided by a three-legged platform which stood on the floor of the plastic tank which housed the water bath. For the experiments in which the axis of the outer cylinder was inclined, the platform was fitted with a ramp-like fixture having an adjustable ramp angle. The volume of the water bath was approximately 200 l, and its temperature rise during a data run was entirely negligible (at most, about 0.02°C).

The Rayleigh number was varied by variations of the temperature difference between the inner and outer cylinders. The overall range of the intercylinder temperature difference extended from 0.75 to 45°C, with a corresponding range of the inner-cylinder Rayleigh number from 1500 to 90 000. To cover the desired range of the geometrical parameters and the Rayleigh number, well over 100 data runs were made, including verification runs.

Data reduction

The average heat transfer coefficient and Nusselt number for the inner cylinder (subscript i) were evaluated from

$$h_i = Q_{conv}/A_i(T_i - T_o), \quad Nu_i = h_i D_i/k, \tag{1}$$

where $(T_i - T_o)$ is the intercylinder temperature difference, and Q_{conv} is the rate of convective heat transfer. Furthermore, since the cylinder length and diameter are equal, $A_i = (3/2)\pi D_i^2$. The only modifications needed to evaluate h_o and Nu_o (outer-cylinder parameters) are to change the surface area and diameter in equation (1). This yields

$$Nu_o = 0.2Nu_i, \tag{2}$$

which follows because the diameter ratio is 0.2. The results will be reported in terms of Nu_i, and Nu_o can be obtained from equation (2), if desired.

The convective heat transfer Q_{conv} was evaluated from the measured electric power supplied to the inner-cylinder heater, to which a subtractive radiation correction was applied in the form

$$Q_{rad} = \varepsilon_i A_i \sigma (T_i^4 - T_o^4). \tag{3}$$

Equation (3) corresponds to the radiative heat loss at a small body in a large isothermal-walled enclosure.

Owing to the low value of the emissivity ε_i for highly polished aluminum ($\varepsilon_i = 0.05$), Q_{rad} was found to be about 5% of the electric power input. Deviations of the radiative heat transfer model from reality would tend to decrease Q_{rad}, but since Q_{rad} is already small, such deviations should have a negligible effect on Q_{conv}.

The Nu_i results will be parameterized by the inner-cylinder Rayleigh number Ra_i

$$Ra_i = [g\beta(T_i - T_0)D_i^3/\nu^2]\,Pr. \quad (4)$$

The mean temperature $\frac{1}{2}(T_i + T_0)$ was used as the reference temperature T_r for the air properties that appear in equations (1) and (4), with $\beta = 1/T_r$. For the density evaluation, the barometric pressure was employed since the experimental procedure gave rise to pressure equality between the intercylinder enclosure and the ambient.

RESULTS AND DISCUSSION

Results for the inner-cylinder Nusselt number Nu_i are presented in Figs. 3–5. In these figures, Nu_i is plotted as a function of Ra_i over the range from 1500 to 10^5. The various sets of data appearing in these figures are parameterized by the inner-cylinder position coordinates X_c/L and Z_c/H and by the orientations of the outer cylinder. These orientations are identified as cases (a)–(c), respectively depicted in Figs. 1(a)–(c). A special focus of Figs. 3–5 is the comparison of the Nu_i values for the various inner-cylinder positions and outer-cylinder orientations.

Figure 3 conveys results for case (b) (i.e. outer cylinder oriented with its axis horizontal), with the inner cylinder centered between the horizontal extremities of the outer cylinder—$X_c/L = 0$. The figure contains four tiers of data, the upper three of which correspond to the three investigated inner-cylinder elevations, $Z_c/H = 0.1375, 0.5$, and 0.8625. In the lower portion of the figure, the data for all elevations are brought together and compared. Each tier of data has its own ordinate scale, while all share a common abscissa. The open data symbols represent the present Nu_i results, while the black circles correspond to the data for case (a), taken from ref. [3].

Attention is first focused on the comparison between the present data [case (b)] and those of ref. [3] [case (a)], as shown in the upper three tiers of Fig. 3. This comparison, made at $X_c/L = 0$, appears apt because in both cases the inner cylinder is positioned at the horizontal midpoint of the enclosure. However, the enclosure has a different shape in the two cases (when viewed with respect to the gravity vector), and differences in the patterns of flow circulation in the enclosure are to be expected.

Despite this expectation, the agreement between the two sets of data is remarkably good. The extreme deviation is about 5%, which occurs at two points in the lower Rayleigh number range at the mid-height elevation. Aside from these, virtually perfect agreement prevails, especially at higher Rayleigh numbers.

Next, consideration is given to the comparison of the data for the various elevations that have been brought together in the lower part of Fig. 3. Inspection of the data shows complete insensitivity to elevation at the higher Rayleigh numbers. However, as the Rayleigh number decreases, the data for the mid-height position tend to drift below those for the highest and lowest elevations, which continue to be in perfect agreement for the entire range. The largest spread between the mid-height data and the others is in the range of 10–15%.

The aforementioned higher Nusselt numbers at the

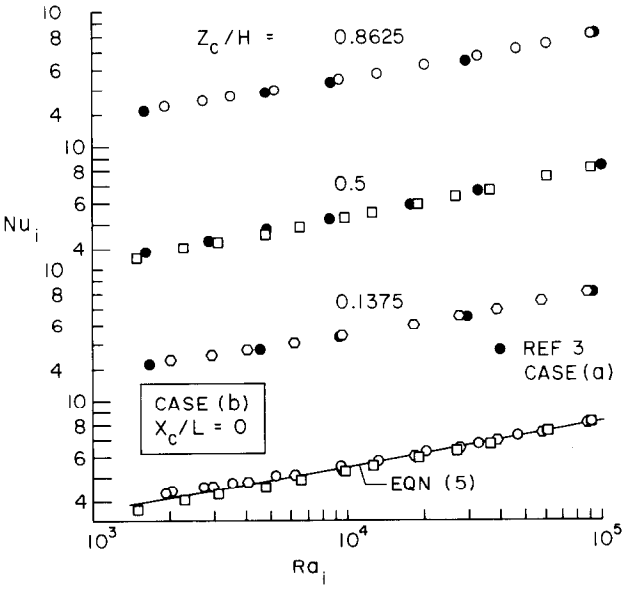

FIG. 3. Nusselt number results for case (b) of Fig. 1 with $X_c/L = 0$.

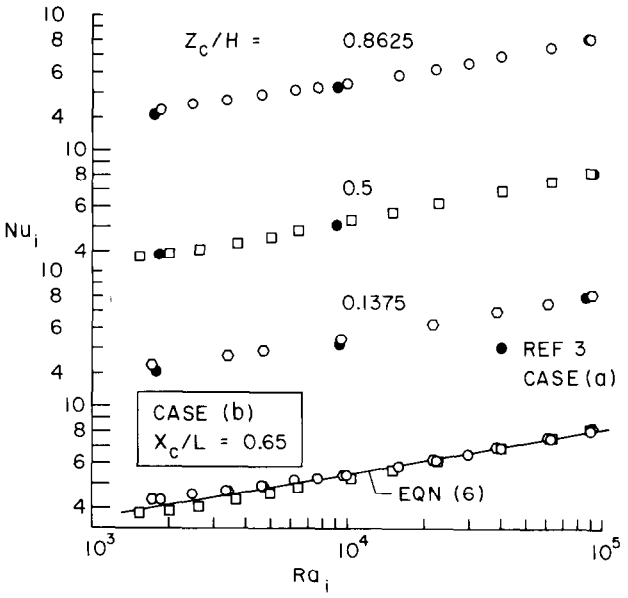

FIG. 4. Nusselt number results for case (b) of Fig. 1 with $X_c/L = 0.65$.

uppermost and lowermost elevations can be attributed to short-range heat conduction between the inner and outer cylinders, owing to their close proximity. The importance of this short-range conduction is heightened at low Rayleigh numbers, where natural convection is relatively weak. Such direct conduction does not operate when the inner cylinder is relatively far from the outer cylinder, as in the mid-height position.

The data assembled in the lower part of Fig. 3 have been fit with a least-squares power law whose equation is

$$Nu_i = 1.077 Ra_i^{0.176}. \quad (5)$$

A straight line representing equation (5) has been plotted in the figure. At the higher Rayleigh numbers, the correlating line threads neatly through the tightly compacted data, while in the lower range, it tends to split the difference between the mid-height data and those at the extreme positions. The maximum deviations between the line and the data are about $\pm 6\%$ and occur at the lowest of the investigated Rayleigh numbers. The 0.176 exponent appearing in equation (5) is lower than that for external natural convection flows in this range of Rayleigh number.

Figure 4 presents results for case (b) with the inner cylinder positioned at $X_c/L = 0.65$. This case is

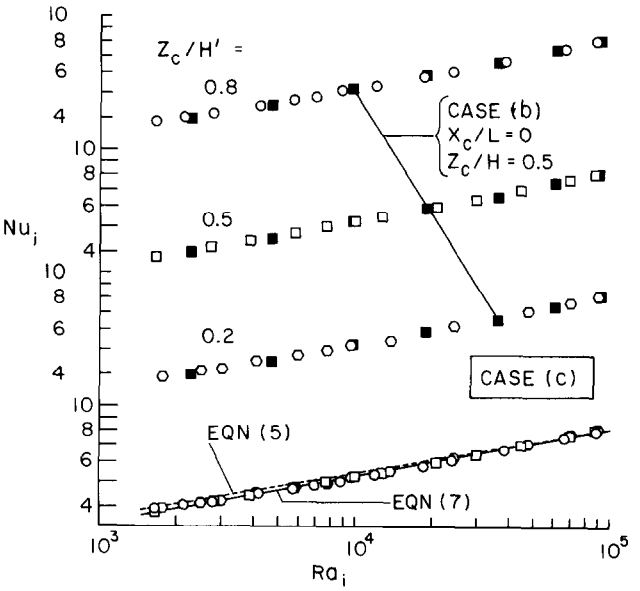

FIG. 5. Nusselt number results for case (c) of Fig. 1.

depicted in Fig. 1(b). Relative to the just-discussed $X_c/L = 0$ case, the inner cylinder is now much closer to the end wall of the outer cylinder. Also plotted in Fig. 4 are the data from ref. [3] which correspond to $X_c/L = 0.65$ for case (a) [Fig. 1(a)]. Thus, both the present results and those of ref. [3] correspond to the same nominal horizontal position of the inner cylinder, i.e. centered at 65% of the distance between the horizontal mid-point and the horizontal extremity of the outer cylinder. However, the surfaces of the two cylinders which are in close proximity are not the same in the two cases and, also, the general flow circulation in the enclosure should be different because of the different orientations of the outer cylinder.

The format of Fig. 4 is identical to that of Fig. 3, with the data for each of the three elevations, $Z_c/H = 0.1375$, 0.5, and 0.8625, stacked one above the other. In the lower part of Fig. 4, the data for all the elevations are brought together and compared.

Inspection of Fig. 4 shows that there is generally good agreement between the results for cases (a) and (b). The largest deviations, about 5%, occur at the lowest Rayleigh number for the uppermost and lowermost elevations. These deviations are believed to be due to differences in the direct intercylinder heat conduction for the two cases.

The data collected in the lower part of Fig. 4 display trends that are remarkably similar to those of Fig. 3—virtual coincidence of all the data at the higher Rayleigh numbers and a gradual drift of the mid-height data below the others at lower Rayleigh numbers. The collected data have been fit with the least-squares line

$$Nu_i = 1.116 Ra_i^{0.172}, \tag{6}$$

with maximum data deviations of $\pm 7\%$. It is also relevant to take note of the fact that equations (5) and (6) are within 1% of each other over the investigated range, $1500 \leqslant Ra_i \leqslant 10^5$. This finding demonstrates the remarkable and surprising insensitivity of the Nusselt number results to the horizontal positioning of the inner cylinder within the enclosure.

Attention is next directed to the results for case (c) as presented in Fig. 5. From Fig. 1, it may be seen that case (c) can be arrived at by starting with the inner cylinder at the $X_c/L = 0.65$ position for case (b) and then tilting the axis of the outer cylinder upward and to the right at an angle of 45°.

The wall-to-wall plumb-line distance H' shown in Fig. 1 is equal to $1.145H$. The upper and lower inner-cylinder positions, $Z_c/H' = 0.2$ and 0.8, were chosen to achieve a close approach of the corner of the inner cylinder to the adjacent wall of the outer cylinder. For $Z_c/H' = 0.2$, the adjacent wall is a flat surface, while for $Z_c/H' = 0.8$, the adjacent wall is a curved surface.

The multi-tiered format of Fig. 5 is similar to that of the previous figures. There is, however, a major difference between Fig. 5 and its forerunners. Whereas in both Figs. 3 and 4 there was a logical comparison to be made with data from ref. [3] [i.e. case (a)], no such comparison suggests itself for Fig. 5. Instead, a comparison is made with the data for the mid position of case (b), i.e. $X_c/L = 0, Z_c/H = 0.5$. These comparison data are depicted by filled squares and are plotted in all of the three uppermost tiers of Fig. 5.

By inspection of Fig. 5, it is seen that excellent agreement prevails between the comparison case and all three Z_c/H' positions of case (c). To illuminate this outcome, it is relevant to note that the comparison case is one where direct intercylinder conduction does not occur since the two cylinders are relatively remote from each other. The same situation prevails for the $Z_c/H' = 0.5$ position of case (c). For the lower and upper positions of case (c), there is close proximity of a corner of the inner cylinder to the adjacent wall of the outer cylinder, but away from the corner region direct conduction should not play an important role. Therefore, since direct conduction is not a factor in the comparison and since virtually perfect agreement is in evidence, it may be concluded that the average inner-cylinder Nusselt number is insensitive to the specifics of the interaction between the inner cylinder and the general recirculation in the enclosure.

The data for the three Z_c/H' positions for case (c) are collected in the lower part of Fig. 5, where near-perfect agreement is seen to prevail. The solid line passing through these data is a least-squares fit whose equation is

$$Nu_i = 0.9390 Ra_i^{0.188}, \tag{7}$$

with a maximum deviation of $\pm 3\%$. Also plotted as a dashed line in Fig. 5 is equation (5), which represents the least-squares fit for the three Z_c/H positions at $X_c/L = 0$ for case (b). Equations (5) and (7) are virtually coincident at higher Rayleigh numbers but deviate slightly at lower Rayleigh numbers. These deviations occur because equation (5) includes the effect of short-range conduction at the upper and lower positions, while these effects do not occur in the case that is correlated by equation (7). The maximum deviation occurs at the lowest investigated Rayleigh number ($Ra = 1500$) and is only 5%.

The general insensitivity of the inner-cylinder Nusselt number to inner-cylinder position and to outer-cylinder orientation in the gravity field motivates a Nu_i, Ra_i least-squares fit of all the data. To this end, the 103 data points from the present investigation and 42 data points from ref. [3] were brought together, which gave

$$Nu_i = 1.050 Ra_i^{0.178}. \tag{8}$$

Half of the data points fall within $\pm 2\%$ of equation (8), and 81% of the data fall within $\pm 4\%$. All but one of the data points lie within a band $+6.5$ to -5.3% about equation (8).

It is interesting to compare the correlation equation (8) with a correlation equation quoted in ref. [3] which is based on numerical finite difference solutions of the conservation equations for mass, momentum, and energy

$$Nu_i = 0.820 Ra_i^{0.204}. \tag{9}$$

Owing to the complexity of the problem, the numerical solutions were limited to the axisymmetric version of case (a) (i.e. $X_c/L = 0$). Also, the solutions were confined to the range $0.25 \leqslant Z_c/H \leqslant 0.75$, so that the effects of short-range intercylinder conduction were probably not significant.

Over the range $1500 \leqslant Ra_i \leqslant 10^5$, the deviations between equations (8) and (9) do not exceed $5\frac{1}{2}\%$. The empirical correlation (8) is recommended for use in applications since it is based on a much wider range of geometrical conditions than is equation (9).

CONCLUDING REMARKS

The experimental data presented here have demonstrated that the average Nusselt number for a small innerbody situated in an enclosed space is quite insensitive to the position of the innerbody and to the orientation of the enclosure in the gravity field. In the present experiments, the enclosure was a cylindrical space of equal length and diameter, while the innerbody was also a cylinder whose length was equal to its diameter. The ratio of the diameter (length) of the inner cylinder to the diameter (length) of the outer cylinder was 0.2.

The results indicate that the Nusselt number can be affected by direct conduction between the innerbody and the bounding wall of the enclosure when the gap between them is very small. This effect was found to become more important at low Rayleigh numbers, where natural convection is relatively weak. The maximum conduction-related enhancement encountered here was in the 10–15% range and occurred at the lowest of the investigated inner-cylinder Rayleigh numbers (~ 1500). Above a Rayleigh number of 10^4, the direct-conduction effect was negligible.

It is to be expected that the recirculating flow in the enclosure is affected by the orientation of the enclosure in the gravity field. Furthermore, the numerical solutions quoted in ref. [3] indicate that the large-scale features of the recirculation are also affected by the position of the inner cylinder in the enclosure. Notwithstanding these happenings, the average inner-cylinder Nusselt number is virtually unaffected by the enclosure orientation or inner-cylinder position (except for the short-range heat conduction discussed in the preceding paragraph). From this, it may be concluded that the velocity and temperature fields in the enclosure proper form a benign backdrop which has a hardly discernible influence on the velocity and temperature fields in the region immediately adjacent to the surface of the inner cylinder.

The foregoing realization about the benign nature of the enclosure fields suggests a further generalization of the results—namely, that the Nu_i, Ra_i relationship obtained from the present experiments should apply with acceptable accuracy for inner-cylinder–outer-cylinder diameter (length) ratios less than 0.2. This expectation is supported by the finite difference solutions quoted in ref. [3] [case (a), $0.25 \leqslant Z_c/H \leqslant 0.75$]. Those solutions show an increase in Nu_i of only 3.6% as the diameter ratio decreases from 0.2 to 0.1. It is, therefore, recommended that equation (8) be employed for diameter ratios of 0.2 and less.

As a final matter, it is relevant to inquire about how the percent findings relate to those of refs. [1, 2], where off-center innerbodies were also investigated. For the eccentric spheres studied in ref. [1], the average heat transfer coefficients exceeded those for the concentric case, but the extent of the enhancement could not be identified because of the particular nature of the correlation of the results. The eccentric horizontal annulus studied in ref. [2] yielded average heat transfer coefficients that differed by no more than 10% from the concentric case, thereby reinforcing the findings of the present investigation.

REFERENCES

1. N. Weber, R. E. Powe, E. H. Bishop and J. A. Scanlan, Heat transfer by natural convection between vertically eccentric spheres, *J. Heat Transfer* **95**, 47–52 (1973).
2. T. H. Kuehn and R. J. Goldstein, An experimental study of natural convection heat transfer in concentric and eccentric horizontal cylindrical annuli, *J. Heat Transfer* **100**, 635–640 (1978).
3. E. M. Sparrow and M. Charmchi, Natural convection experiments in an enclosure between eccentric or concentric vertical cylinders of different height and diameter, *Int. J. Heat Mass Transfer* **26**, 133–143 (1983).

CONVECTION NATURELLE DANS DES ENCEINTES AVEC DES CORPS INTERIEURS DECENTRES

Résumé—Des mesures sont effectuées pour le nombre de Nusselt moyen relatif à un petit corps interne situé dans un espace clos, avec le corps interne et la paroi de l'enceinte maintenus à des températures uniformes différentes. La convection naturelle s'établit dans l'air qui remplit l'espace intermédiaire. La position du corps interne dans l'enceinte est rendue variable, de même que l'orientation de l'enceinte par rapport au champ de gravité. Le corps interne et l'enceinte sont des cylindres avec des rapports longueur-diamètre égaux à l'unité et le rapport des diamètres est 0,2. Aux faibles nombres de Rayleigh et pour des espaces étroits entre le corps et l'enceinte, une conduction directe entre parois accroît le nombre de Nusselt du corps interne. A coté de cela, le nombre de Nusselt est remarquablement insensible à la position du corps interne et à l'orientation de l'enceinte. Les résultats sont représentés à $\pm 6\%$ par la relation $Nu_i = 1{,}050 Ra_i^{0.178}$.

FREIE KONVEKTION IN HOHLRÄUMEN MIT AUSSERMITTIGEN, INNENLIEGENDEN KÖRPERN

Zusammenfassung—An einem kleinen Körper, der sich in einem abgeschlossenen Raum befand, wurde die mittlere Nusselt-Zahl gemessen, wobei der Körper und die umschließende Wand auf unterschiedlichen konstanten Temperaturen gehalten wurden. Im Zwischenraum, der mit Luft gefüllt war, trat freie Konvektion auf. Die Lage des Körpers innerhalb des Hohlraums wurde als Parameter variiert, ebenso die Orientierung des Hohlraums im Bezug zum Schwerefeld. Sowohl der innere Körper als auch der Hohlraum waren Zylinder mit einem Verhältnis von Länge zu Durchmesser von eins. Das Verhältnis der beiden Durchmesser zueinander war 0,2. Bei kleinen Rayleigh-Zahlen und für enge Spalte zwischen dem inneren Körper und der umgebenden Wand des Hohlraums vergrößerte direkte Wärmeleitung zwischen den Wänden die Nusselt-Zahl am inneren Körper. Abgesehen davon, war die Nusselt-Zahl sowohl gegenüber der Lage des inneren Körpers und der Orientierung des Hohlraumes bemerkenswert unempfindlich. Die Ergebnisse lassen sich innerhalb $\pm 6\%$ Fehlergrenze durch die Beziehung $Nu_i = 1{,}050 Ra_i^{0{,}178}$ wiedergeben.

ЕСТЕСТВЕННАЯ КОНВЕКЦИЯ В ПОЛОСТЯХ, СОДЕРЖАЩИХ НЕЦЕНТРАЛЬНО РАСПОЛОЖЕННЫЕ ТЕЛА

Аннотация—Измерены средние значения числа Нуссельта для тела небольших размеров, находящегося внутри замкнутой полости, когда тело и стенки полости поддерживаются при разных, но постоянных температурах. Естественная конвекция происходит в воздухе, заполняющем межцилиндрическое пространство. Как положение тела в полости, так и ориентация полости изменялись параметрически относительно направления поля силы тяжести. Тело и полость имели цилиндрическую форму с отношениями длины к диаметру, равными единице, и отношением диаметров цилиндров, равным 0,2. При малых значениях числа Рэлея и небольших зазорах между телом и полостью число Нуссельта для тела возрастало за счет теплопроводности между стенками тела и полости. Кроме того, число Нуссельта не зависит ни от положения тела, ни от ориентации полости. Результаты обобщены с точностью $\pm 6\%$ зависимостью вида $Nu_i = 1{,}050\ Ra_i^{0{,}178}$.